Food Control 142 (2022) 109239

Contents lists available at ScienceDirect

Food Control

journal homepage: www.elsevier.com/locate/foodcont

Near-infrared hyperspectral imaging evaluation of *Fusarium* damage and DON in single wheat kernels

Antoni Femenias, Enric Llorens-Serentill, Antonio J. Ramos, Vicente Sanchis, Sonia Marín *

Applied Mycology Unit, Food Technology Department, University of Lleida, AGROTECNIO-CERCA Center, Av. Rovira Roure 191, 25198, Lleida, Spain

A B S T R A C T

Fusarium is a DON producing filamentous fungus which commonly infects small grain cereals. Near-Infrared Hyperspectral Imaging (HSI-NIR) is considered for its potential to manage this contamination, as it uses spatial recognition, which may be able to deal with the heterogeneity inside the batches for cereal sorting implementation. The focus of this study was the application of HSI-NIR for *Fusarium* Damaged Kernels (FDK) detection and DON prediction and discrimination of wheat kernels over EU limit. After the HSI scanning of 300 individual grains, the reference values were obtained attributing categories for typical fungal symptoms and analyzing DON from individual grains by HPLC. Several spectral preprocessing methods selected valuable information before model calibration. Externally validated PLS predictions showed RMSEP of 6.65 mg/kg, an R^2 of 0.88 and an RPD of 3.21. However, the classification models managed wheat contaminations more appropriately, obtaining discrimination accuracies of 85.8% and 76.9% for fungal symptoms and DON at the EU limit, respectively. These findings suggest that HSI-NIR can be a suitable tool to sort DON contaminated kernels at EU limit.

1. Introduction

Fusarium is a well-known plant-pathogen fungus associated with small grain cereal diseases, such as Fusarium Head Blight (FHB), which grows in favourable moist and warm conditions. Its infection is related to yield and grain quality reduction with the appearance of *Fusarium* damaged kernels (FDK). The main changes produced in FDK are shrivelling, weight loss, and discolouration. From a food safety perspective, *Fusarium graminearum* and *F. culmorum* can produce mycotoxins, in which deoxynivalenol (DON) is the most common. This secondary metabolite is associated with human and livestock health problems. Acute and chronic disorders are attributed to DON through cereal consumption (Sudakin, 2003), thus exposure to a cereal-based diet, and the increased incidence of mycotoxins due to climatic change (Marroquín-Cardona, Johnson, Phillips, & Hayes, 2014) can increase the risk of developing an associated disease. Consequently, food safety authorities have established a maximum limit of DON for unprocessed wheat in 1750 μg/kg for durum wheat and 1250 μg/kg for cereals other than durum wheat, oats, and maize (European Commission, 2006a).

Conventional analysis techniques, such as Enzyme-linked immunosorbent assay (ELISA), High-Performance Liquid Chromatography (HPLC) and High-Performance Liquid Chromatography – Mass Spectrometry (HPLC-MS), and immunochromatographic strips, for DON detection, have been frequently applied before the cereal entrance in the food industry. The official controls of mycotoxins levels (European Commission, 2006b) attempt to represent, as far as possible, the contamination of the entire batch. Nevertheless, even if a suitable sampling protocol is applied, enough representation of the lot is not reached, and few extremely-contaminated kernels can disrupt the admission of the whole batch associated with a loss in the production yield and a negative economic impact. The heterogeneous distribution of the contaminated grains is an issue in the cereal batches. Some kernels suffer fungal infection (with or without associated DON presence) inside the sample, while the rest can remain healthy (Champeil, Fourbet, & Doré, 2004; Delwiche, Pearson, & Brabec, 2007). Besides, the above-mentioned traditional techniques are expensive, time-consuming, and sample destroying. Companies require new methods able to sort mycotoxin contaminated kernels overcoming batch heterogeneities.

In some studies, authors used FDK as DON presence indicators (Delwiche, Kim, & Dong, 2011; Dowell, Ram, & Seitz, 1999; Jin et al., 2014). However, Paul, Lipps, and Madden (2005) obtained a correlation of 0.73 between FDK and DON. Moreover, Barbedo, Tibola, and Fernandes (2015) used an algorithm based on a *Fusarium* index (probability of a kernel of being infected with FHB based on visual inspection) that presented a correlation of 84% with DON. It also demonstrated that correlations found for high DON levels were substantially higher than for low DON concentrations. Although they reached positive correlations, the indirect determination of DON using FDK would drag consecutive errors that would affect the reliability of the results.

Single-kernel NIR (SK-NIR) has been used for *Fusarium* detection in wheat by Polder, van der Heijden, Waalwijk, and Young (2005), which

* Corresponding author. Food Technology Department, University of Lleida, Av. Rovira Roure 191, 25198, Lleida, Spain.
E-mail address: sonia.marin@udl.cat (S. Marín).

https://doi.org/10.1016/j.foodcont.2022.109239
Received 18 January 2022; Received in revised form 3 June 2022; Accepted 6 July 2022
Available online 19 July 2022

Nomenclature

ANN	Artificial Neural Networks
DAD	Diode Array Detector
DON	Deoxynivalenol
ELISA	Enzyme-Linked Immuno-Sorbent Assay
FDK	*Fusarium* Damaged Kernel
FI	*Fusarium* Index
FHB	Fusarium Head Blight
GC-MS	Gas Chromatography – Mass spectrometry
HPLC	High-Performance Liquid Chromatography
HPLC-MS	High-Performance Liquid Chromatography – Mass Spectrometry
HSI-NIR	Near-Infrared Hyperspectral imaging
K-NN	K-Nearest Neighbours
LDA	Linear Discriminant Analysis
LMT	Logistic Model Tree
MLP	Multilayer perception
MSC	Multiplicative Scatter Correction
MSI	Multispectral imaging
NIR	Near-Infrared
PC	Principal Component
PCA	Principal Component Analysis
PLS	Partial Least Squares
PLS-DA	Partial Least Squares – Discriminant Analysis
qPCR	Quantitative Polymerase Chain Reaction
RMSECV	Root Mean Square Error of Cross-Validation
RMSEP	Root Mean Square Error of Prediction
ROI	Region of Interest
RPD	Ratio of Performance to Deviation
RT-PCR	Reverse-Transcription Polymerase Chain Reaction
SAE	Sparse autoencoder
SK-NIR	Single Kernel – Near Infrared
SNV	Standard Normal Variate
SWIR	Short-Wave Infrared
UHPLC	Ultra-High-Performance Liquid Chromatography
UHPLC-DAD	Ultra-High-Performance Liquid Chromatography – Diode Array Detector

used near-infrared technology linked to Reverse-Transcription Polymerase Chain Reaction (RT-PCR) to predict the amount of *Fusarium*. However, most studies with the same objective used the visual inspection of kernel symptoms to typify them as *Fusarium*-damaged or healthy by Near Infrared (NIR) (Delwiche et al., 2011). Some of them also analysed DON in single kernels (Peiris, Bockus, & Dowell, 2016; Peiris et al., 2010) by SK-NIR technology. However, in both studies, artificial inoculation of wheat spikes was performed before GC-MS analysis, achieving kernel discrimination with a DON threshold of 60 mg/kg. Dowell et al. (1999) analysed by SK-NIR using HPLC as the reference method for DON. In their calibration, they removed kernels with contamination >5 mg/kg, for which most of them presented a DON concentration between 50 and 500 mg/kg, a level which differs from those commonly found in naturally contaminated samples. Jaillais, Roumet, Pinson-gadais, and Bertrand (2015) developed SK-NIR multivariate imaging method to detect FHB in wheat kernels. They analysed different trichothecenes-producing fungi with RT-PCR. Then, they calibrated Principal Component Analysis (PCA) models for contaminated grains detection and Partial Least Square (PLS) to map the contaminated regions within the kernels using selected spectral bands.

Researchers used hyperspectral imaging to combine the whole spectra and the spatial resolution, making it appropriate to apply it to single kernel screening. All the studies except one focused on detection of *Fusarium* in wheat single kernels. In most of the works, an inspector examined manually the grains, which added subjectivity to the study. On the other hand, Singh, Jayas, Paliwal, and White (2012) artificially inoculated kernels with fungi before scanning them by HSI-NIR and digital colour imaging. Although the artificial contamination avoided the subjectivity from visual inspection, the controlled inoculation presents differences from natural contamination. Delwiche et al. (2011) calibrated a FHB classification model based on Linear Discriminant Analysis (LDA) using HSI-Vis/NIR on four characteristic wavelengths (502, 678, 1198 and 1496 nm). A second attempt was done (Delwiche, Rodriguez, Rausch, & Graybosch, 2019) but using HSI-NIR (938–1654 nm). They selected four spectral bands (1000, 1197, 1308 and 1394 nm) as the optimum for LDA calibration, although they built an alternative Partial Least Squares – Discriminant Analysis (PLS-DA) model. In addition, Ropelewska and Zapotoczny (2018) classified FHB damaged kernels by testing different mathematical classifiers (Bayes net, LDA, K-Star, Rules PART and Logistic Model Tree (LMT)) for hyperspectral and colour images. Barbedo et al. (2015) also evaluated FHB in SK, which used HSI-Vis/NIR technology to build an algorithm based on the *Fusarium* index (FI). The probability density function based on FI, identifying sound and diseased kernels, was correlated with DON concentration to attempt an indirect estimation of the DON levels. Liang et al. (2018) focused exclusively on the determination of different levels of DON using a complex algorithm. Although they did not analyse single kernels, they built a distribution map discerning heavily infected regions within the bulk samples corresponding to the highly contaminated grains.

This study focused on DON prediction in single wheat kernels by an optimized algorithm and to classify them according to typical visual symptoms caused by *Fusarium* infection and different DON levels according to EU maximum limit. This study is a starting point for HSI-NIR calibration that could at real-time identify and reject damaged or DON contaminated kernels at food industry entrance.

2. Material and methods

2.1. Wheat kernels

A feed-producing agricultural cooperative supplied wheat samples (approximately 500 g of bulk wheat grains) harvested during 2018–2019. The origin of the wheat was the plain area of the Lleida province. A highly contaminated sample was selected, previously analysed twice by Ultra-High Performance Liquid Chromatography (UHPLC) (2682.8 and 2403.5 μg/kg of DON). Three hundred wheat kernels from the sample were selected, including all the typical characteristics of sound and diseased wheat kernels. The kernels had a mean weight of 30.2 mg, ranging from 6.2 to 58.1 mg, and were used for DON prediction and classification according to fungal symptomatology and DON levels.

2.2. HSI-NIR instrumentation and data acquisition

The hyperspectral imaging system was the standardized in a previous study (Femenias, Bainotti, Gatius, Ramos, & Marín, 2021). The raw reflectance readings for each test sample data array were corrected by dividing the dark current-subtracted reflectance by the dark current subtracted white standard reflectance at each of the corresponding wavelengths (1). A dark current intensity image, taken with the covered camera's lens, removed the dark noise. Likewise, a reflectance standard with a 99% intensity made of polytetrafluoroethylene (Spectralon™, SRT-99-120, Labsphere, North Sutton, NH, USA) corrected the illumination effects. These two images were applied to subsequent sample intensity images.

$$I = \frac{I_0 - I_b}{I_w - I_b} \quad (1)$$

where the I is the corrected reflectance intensity, I_0 the raw hyperspectral image intensity, I_w the white reference intensity and I_b the dark current reference intensity. In addition to the dark current, the camera controls permitted the adjustment of the pixel illumination saturation. The configuration of the framerate and the integration time avoided pixel saturation.

The hyperspectral system acquired data for 300 kernels in the laboratory to calibrate the predictive and classification models. From the 300 kernels, spectral data from 180 were used for model calibration and the remaining 120 for the external validation. According to our previous study (Femenias et al., 2021), the analysis was performed for the crease-down side of the kernel, which is more rapidly and easily manipulated and did not show significant differences in results with the crease-up position.

In all the cases, the black tray reduced the background noise in the image to obtain an accurate pixel selection. The image scan had 350 bands on the horizontal size and approximately 90 mm on the vertical. Kernel's pixel data were collected by the mean reflectance and mean first derivative values of similar spectrum pixels calculated by Euclidian distance, which is best adjusted to the ROI to remove the background signal. Individual kernel raw and first derivative spectra were saved as a text file for subsequent exporting to the spectral analysis software.

2.3. DON analysis of wheat kernels by UHPLC

2.3.1. Reagents and chemicals

A Milli-Q® SP Reagent water system from Millipore Corp. (Brussels, Belgium) produced the water used. Methanol and acetonitrile (HPLC grade) were purchased from Scharlab (Sentmenat, Spain). DON standards were obtained from Romer Labs (Tulln, Austria).

2.3.2. Preparation of DON solutions

The DON concentration was checked in the stock solution by UV spectroscopy following the AOAC Official Methods of Analysis, Chapter 49 (AOAC, 2005). The concentration obtained was 7530 μg/mL for the stock solution. Standard solutions of DON were prepared in acetonitrile at a concentration of 10 μg/mL and stored at 4 °C. The calibration curves were prepared by the appropriate dilutions of known volumes of the stock solution with the mobile phase.

2.3.3. DON extraction in wheat kernels

The kernels already analysed by spectroscopy were quantified for DON by UHPLC. The extraction followed the methodology used by Femenias et al. (2021). Concisely, each grain was individually and manually ground with a small laboratory mortar and pestle and mixed with 0.5 mL of MiliQ water in a 1.5 mL Eppendorf tube, followed by 10 min vortexing and 10 min of sonication. Then, samples were centrifuged for 10 min at 1780×*g*. The supernatant was filtered through a nylon filter (0.4 μm) and was evaporated. Finally, the sample was resuspended with 150 μL of mobile phase before being injected into the Ultra-High Performance Liquid Chromatography – Diode Array Detector (UHPLC-DAD) system.

2.3.4. UHPLC system

DON concentrations were obtained using an Agilent Technologies 1260 Infinity UHPLC system (California, USA) coupled with an Agilent 1260 Infinity II Diode Array Detector (DAD). A Gemini® C18 column from Phenomenex 150 × 4.6 mm (California, USA) with a particle size of 5 μm and a pore size of 110 Å was used. The absorption wavelength was set at 220 nm. The mobile phase was composed of methanol:water (10:90, v/v/v) and set at a flow rate of 1 mL/min. The column temperature was 40 °C, the injection volume was 100 μL and the total run time was 15 min for mycotoxin analyses. The performance of the method for the quantification of DON in wheat was tested, in which the limit of detection (LOD: 100 μg/kg) was considered to be three times the signal of the blank.

2.3.5. Prediction and classification modelling of DON for individual kernel analysis (Fig. 1)

Selectivity was checked by injecting 5 μL of standard solution at least three times (150 μg/L) and comparing retention time and peak resolution between injections. For linearity check, a calibration curve of eight concentration levels for DON solutions (20, 30, 50, 100, 250, 500, 1000, 3000 μg/L solutions) was prepared and injected into the system, generating a linear regression plotting solutions' concentration versus peak area. The method performance was assessed according to Commission Regulation (EC) 401/2006 (European Commission, 2006b).

2.3.6. Quantification modelling of DON contamination

Hyperspectral data were modelled with The Unscrambler software (version 7.6 SR1, CAMO, Oslo, Norway, 2001) for DON level prediction. The reflectance data were used as raw data for the calibration of the regression models. Each kernel was scanned three times, recording intensities from 900 hyperspectral images. Once the grains were optically analysed, the DON concentration was determined from each kernel by UHPLC. The contamination of the 300-kernels set ranged from <LOD to 135.73 mg/kg and the mean concentration was 9.02 mg/kg. The mean reflectance intensities of the pixels from each kernel corresponded to the explanatory variables (X) and the DON concentration obtained by UHPLC was the dependent variable (Y). A first modelling screening was performed by the regression of the hyperspectral data versus the reference method by a leave-one-out cross-validation. This approach allowed an overall perspective of the data adjustment by a single sample leaves out of the training set for each *n* iterations. The leave-one-out cross-validation demonstrated the most realistic approximations to the independent set validation. The data size used in this study is sufficiently large to validate the predictive models independently. The data was divided into a calibration set, which consisted of 540 hyperspectral images (3 images of 180 kernels), and a validation set, which included 360 images (3 images of 120 kernels).

Before the predictive models' calibration, spectral preprocessing tools were applied to the raw data to enhance the remarkable information. The transformations applied in The Unscrambler software were first and second 3 and 5-point Savitzky-Golay and Norris Gap derivatives which reduce noise, additive and multiplicative effects. Alternatively, Multiplicative Scatter Correction (MSC) and Standard Normal Variate (SNV) were applied to overcome the non-linearity of light scattering due to the differences in kernels size. Other pretreatments, such as Normalization and Baseline Correction, were also used to obtain balanced variances and to remove baseline noise, respectively. The optimum pretreatment is not the same for all data sets, as it depends on the raw reflectances, absorbances and transmittances, instrument configuration and calibration, goal and sample characteristics. Thus, several spectral pretreatments had been tested followed by the statistical experience. Otherwise, the improvements tested in previous investigations demonstrated non-linearities and noisy regions in the extremes of the spectra. Thus, models on the 1000–1600 nm range were also calibrated.

The information obtained was used to build the predictive model. We considered PLS regression as the most suitable chemometric tool to be used for NIR data calibration, as it is focused on the Y information to obtain better-adjusted models. The performance of the PLS models depended on the parameters obtained in the model calibration steps. The parameters which determine the most suitable model for DON quantifications are the slope, the offset, the coefficient of determination (R^2), the Root Mean Square Error of Prediction (RMSEP), the optimum number of Principal Components (PC) and the Ratio of Performance to Deviation (RPD).

Depending on the RPD values, the models can be categorized as

excellent predictions (RPD >2.5); good (RPD of 2.0–2.5); approximate quantitative predictions (RPD of 1.8–2.0); possibility to distinguish high and low values (RPD of 1.4–1.8); and unsuccessful (RPD <1.40) (Agelet & Hurburgh, 2010). The combination of the RPD values with high slopes and R^2 and low RMSEP and number of PC indicates a high predictive power of the model.

The calibration models were performed for full spectral range (893.1–1731 nm) and extremes removed spectra (1000–1600 nm). A characteristic wavelength extraction for the best-fitted models was performed, to simplify the computational complexity of the models. The optimum bands were higher regression coefficients wavelengths, whose selection reduced data dimensionality with the minimum loss of information. Thus, band selection reduced the model complexity, the computational time and noise. Despite the reduction in data dimensionality, it explained most of DON variability.

2.3.7. Classification modelling of fungal symptomatology and DON contamination

Hyperspectral data from 300 kernels were modelled to discriminate fungal and DON contaminated kernels. Previous to the hyperspectral acquisition, the kernels were visually inspected and categorized as symptomatic (S) (discolouration, weight loss and shrivelled), medium-symptomatic (part of the symptoms) (M) and asymptomatic (A) (no visible symptoms). Then, based on the DON analysis of kernels by UHPLC, they were also categorized as contaminated (C) and non-contaminated (B) according to the threshold established (1250 μg/kg) corresponding to the legal limit of the EU. JMP PRO 15.2 software was used to calibrate the classification LDA, Naïve Bayes, K-Nearest Neighbours (K-NN) and Artificial Neural Networks (ANN) models. The model performances were evaluated by the classification accuracy, expressed in percentage, and the ratio of false negatives, which indicated the introduction of contaminated kernels into the food chain.

3. Results

3.1. DON and weight variability in single kernels

Kernels from the same batch presented broad differences in DON content. DON contamination covered a range from < LOD and 135.7 mg/kg with a mean concentration of 9.02 mg/kg. Fig. 1 shows that 82 kernels were contaminated under the LOD, which represented the 27.3% of the entire set. In addition, 204 grains had a concentration below the EU legal limit (1.25 mg/kg), and 59 kernels over 10 mg/kg, which indicated that the rejection of a wheat batch could be due to a reduced percentage of highly contaminated kernels. The kernels were manually selected to cover the maximum symptomatology range possible. For that reason, wide variability in DON concentration was observed.

Kernel minimum weight was 6.2 mg, while the maximum observed was 58.1 mg. The differences in the kernel weight could be due to changes produced by fungal growth on the kernel. DON concentrations for kernels lighter or heavier than 30 mg demonstrated that the differences in kernel weight are associated with DON, presenting the light a mean concentration of 2.4 mg/kg and the heavy 15.5 mg/kg. The weights with higher frequencies were the kernels between 20 and 30 mg, as is reported in Fig. 1.

3.2. Spectral profile comparison of FDK and DON affected kernels

The 1st derivative spectra in the NIR region were compared to detect differences in bands caused by *Fusarium* growth and mycotoxin contamination. From the spectral region used (895–1728 nm), the predominant changes were in the range between 1100 and 1450 nm, which could be due to the differences produced by the fungal primary or secondary metabolism. Fig. 2 shows the differences in the 1st derivated mean spectral profile of the (A) sound, mildly symptomatic and FDK and (B) DON kernel contamination above and below 1.25 mg/kg. The

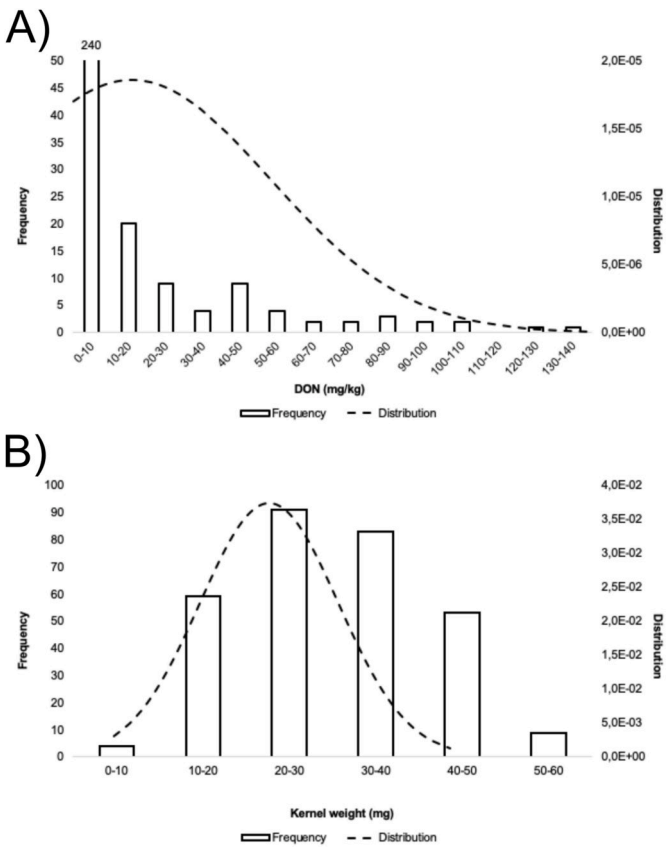

Fig. 1. Distribution of DON content and kernel weight in 300 single wheat kernels dataset. (A) Total kernel DON frequency (in number of kernels) and distribution. (B) Total kernel weight frequency (in number of kernels) and distribution

spectral bands around 1146 nm, 1220 nm, 1350 nm and 1406 nm showed differences between the mean of FDK and healthy kernels and DON high and low contaminated seeds. The use of differences in characteristic spectral peaks for contamination detection was not possible due to the high amount of data to be managed and the overlapping in specific bands. Therefore, the applied chemometric tools resolved the overlapping problems of NIR spectra. In addition, they highlighted the valuable information to build predictive and classification models presented in the following sections.

3.3. DON quantification of SK by HSI-NIR

For DON quantification, data pre-processing improved the model performances. The results presented correspond to the different spectral pre-treatments and entire or extreme-reduced spectra. Table S1 includes the PLS parameters for all data pre-processing methods and validation options. Despite the models calibrated presented similar results, some of them obtained better adjustments due to the spectral pre-treatment. SNV and MSC pre-treated models had the highest performance in cross-validation and external validation procedures. Nevertheless, the models calibrated on SNV transformed spectra presented slightly better adjustment with a RMSEP of 6.66 mg/kg, an R^2 of 0.88 and an RPD of 3.21 by 14 PC calibration, as indicated in Fig. 3.

For the model selected (Fig. 2, Model B), 11 characteristic wavelengths were the spectral bands with higher regression coefficients. Thus, the model is reduced from the hyperspectral dimension to multispectral to reduce model complexity. The bands were 1067, 1159, 1193, 1222, 1252, 1343, 1363, 1378, 1399, 1497, 1554 nm. The model calibrated with those variables was adjusted with a R^2 of 0.84 and a RMSEP of 7.86 mg/kg and RPD of 2.72 with 10 PC. For both models, RPD was

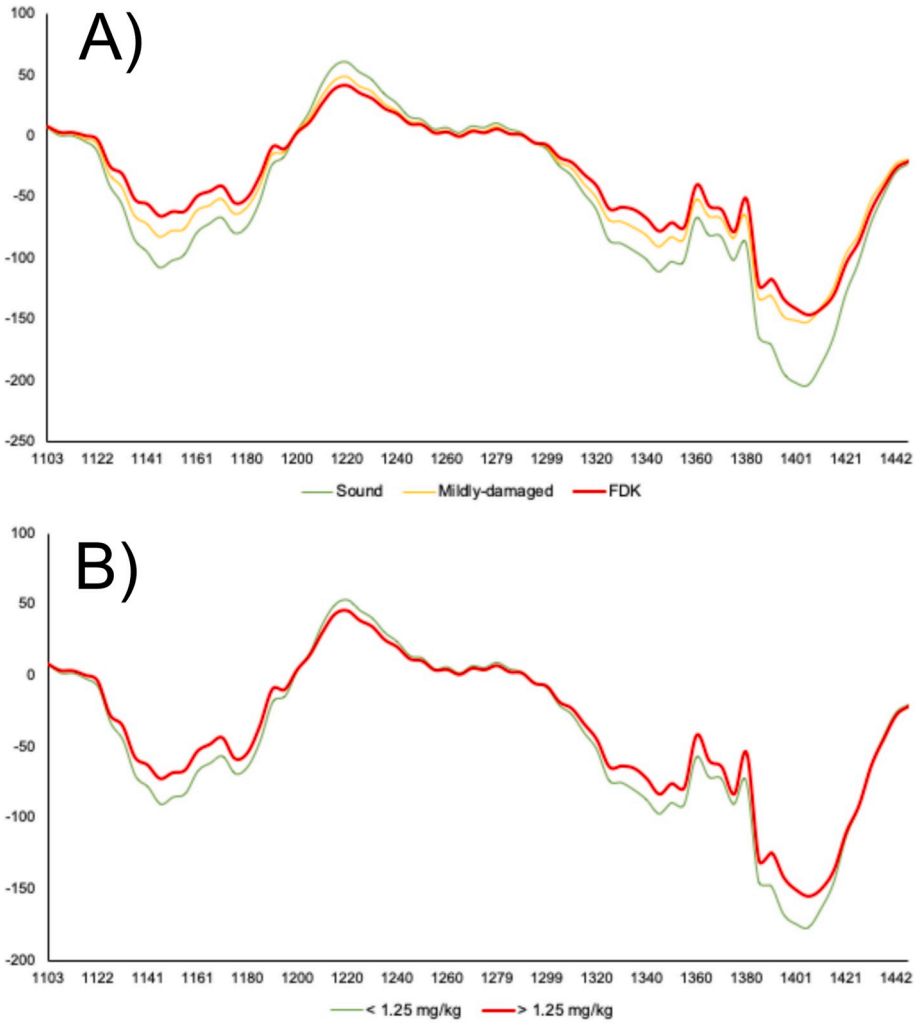

Fig. 2. Mean 1st derivated spectral profile of the (A) difference between FDK (red/bold), mildly-damaged (yellow/semi-bold) and healthy kernels (green/light) and (B) DON contaminated above (red/bold) and below (green/light) 1250 μg/kg.

higher than 2.5, which indicated that the models could predict DON concentrations adequately.

3.4. Classification of SK according to symptomatology by HSI-NIR

HSI was used to discriminate kernels according to the symptoms of fungal infection. The grains were categorized as symptomatic, mildly-symptomatic and asymptomatic depending on the visual inspection of symptoms. The classifiers used to discern between classes were LDA, Naïve-Bayes, K-NN and ANN. The percentage of correctly classified kernels evaluated the discrimination accuracy of the models among the three categories. Table 1 indicates the classification accuracies for each pre-treatment and classifier; the overall results ranged from 57.2 to 85.8%. The pre-treatment which led to better discrimination was the normalization with a mean overall accuracy of 82.4%. However, the classifier that obtained the best accuracy in kernel separation was the ANN, with a percentage of 82.2%. The classification model that showed the maximum accuracy was the ANN using the spectra transformed to absorbance (85.8%). However, normalized spectra modelled with ANN and absorbance baseline-corrected spectra with LDA also presented high-accurate results, obtaining 85.3% and 82.8% of accuracy, respectively. The differences between the results for the whole spectral range and the extreme-reduced spectra were not remarkable. Nevertheless, in some cases, the entire spectral range accuracies were higher.

3.5. Classification of SK according to DON by HSI-NIR

In some cases, changes produced on the kernel due to fungal growth do not imply an increased level of mycotoxins in the product. The classification according to DON levels was challenging due to batch contamination heterogeneity and the discordance between the fungal growth and the mycotoxin contamination. DON was over the legal limit in symptomatic kernels (excluding mildly symptomatic ones) or under the legal limit in asymptomatic or mildly symptomatic ones in 70.7% of the cases. For the remaining 29.3%, DON was present between LOD and the legal limit in symptomatic kernels (20.7%), while the 8.6% had high DON concentrations without presenting visual symptoms.

Table 2 contains the discrimination accuracy of single wheat kernels according to the level of contamination (above and below 1250 μg/kg). For DON discrimination, classification accuracies ranged between 65.0% and 76.9%. The most accurate model was the ANN classifier, with a 73.2% of mean correctness. In addition, the results for the MSC and SNV pre-treated spectra had the highest mean accuracies compared with the other pre-treatments. The most accurate model obtained was the ANN classification with SNV, with an accuracy of 76.9%. However, other models also achieved discriminations above the 76.0%, as Naïve Bayes model with SNV application (76.4%), Naïve Bayes and ANN from the MSC transformed spectra (both 76.1%), ANN for MSC transformed full spectral range (76.4%), and ANN calibration with SNV and 1st derivative application (76.1%). In this case, the differences between the

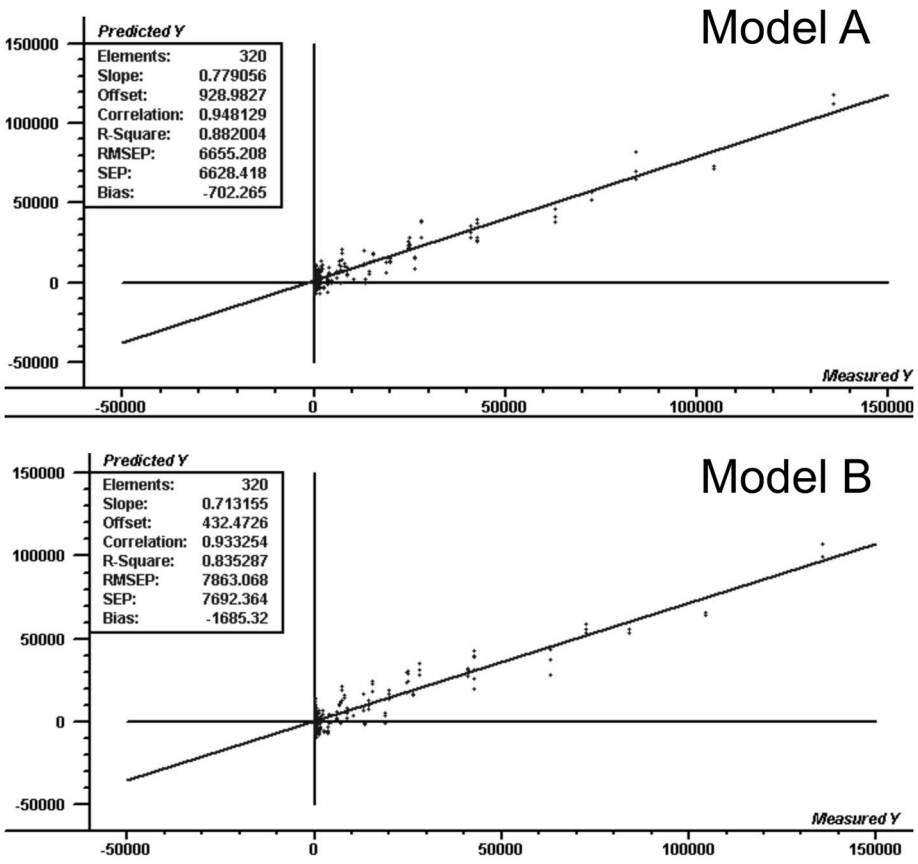

Fig. 3. PLS regression predicted vs. measured plot for independent set validation. Model A: SNV pretreated 1000–1600 nm spectra; optimum number of PC = 14. Model B: SNV pretreated 11 characteristic wavelengths; optimum number of PC = 10.

entire spectral range and the extreme reduced spectra calibrations were not significant. Nevertheless, most of the best results obtained in this section are using the spectra with the extremes removed.

4. Discussion

The analysis of DON content from individual kernels revealed the heterogeneity of the wheat batches. An 80% of the 300-kernel set used in this study had a level of contamination below 10 mg/kg. Moreover, 204 kernels (68%) had a concentration below the legal limit set by the EU (1.25 mg/kg). It indicates that a part of the set (20%), with extreme high contaminations up to 135.7 mg/kg, is responsible for entire batch rejections. Thus, removing the high-contaminated kernels would mitigate DON presence and avoid whole batches rejection and ensure low DON levels in the accepted fraction to reduce harmful health effects and economic losses to producers.

The weight of the grain is also an interesting parameter in the discrimination of the high-contaminated kernels. The mean DON concentration of kernels weighing more than 30 mg was 2.4 mg/kg, while the level in tiny grains lower than 30 mg was 15.5 mg/kg. These differences suggest that weight is correlated with fungal symptomatology and DON production, as the common fungal infection effects include weight loss and shrivelling caused by moisture decrease. NIR data contains the physicochemical changes produced on the sample and can manage kernel size variations to obtain also an effect on the analytical information correlated, in part, by fungal and DON contaminations.

The low correlation between kernels with characteristic visual symptoms and their DON contamination does not avoid the characterization of DON content considering the physical characteristics of the grains. As DON is synthesized as a product of the secondary metabolism of fungi, the amount of fungal growth does not match with the level of contamination. However, even if there are no visible physical changes on the kernels, DON contamination could be modelled by the chemical and nutritional modifications produced by fungal growth on the surface or inner parts of the grains. It includes sugar and free fatty acids content reduction, protein modifications and new fungal metabolites, such as chitin, ergosterol and antibiotics (Sauer, 1988). Then, NIR spectra include all the chemical information of the ROI, which has to be modelled to extract the information required.

The predictive models can be calibrated for more than one chemical compound. The reference values of the compound of interest are required to obtain predictive models to quantify chemicals by spectroscopic analysis. Consequently, authors use multivariate regression methods to deal with the complexity of the NIR data to build well-fitted predictive models. Several published studies aimed to quantify mycotoxins in wheat batches, but only a few tried to use the spatial ability of HSI for the same purpose in individual kernels. First, conventional NIR techniques attempted DON detection in single grains.

One of the first studies regarding DON prediction in single wheat kernels published by Dowell et al. (1999) obtained a prediction error for external validation of 54 mg/kg, including a weak adjustment of data (R^2 of 0.66). The performance was far away from the common DON contamination as they only used scab-damaged kernels with a DON range between 0 and 400 mg/kg. Despite Dowell et al. (1999) worked on 114 single grains for DON assessment, they used only highly contaminated grain above 5 mg/kg. Even using high contaminations, which ideally would obtain the best adjustments than working on low contaminated samples, the coefficient of determination was 0.64 and the standard error 44 mg/kg. Thus, they concluded that NIR spectrometry is unsuitable for this aim. As demonstrated in the study of Peiris et al. (2010), the results improved while working on high levels of contamination from artificially inoculated kernels (>60 mg/kg), obtaining a R^2

Table 1
External validation accuracies of single wheat kernels discrimination according to symptomatology.

	Spectral range	LDA	Naïve Bayes	K-NN	ANN	Mean
Raw spectra	900–1730	76.1	60.6	83.3	84.8	76.3
	1000–1600	77.5	60.3	84.2	83.6	
1stD	900–1730	75.8	78.1	76.9	83.3	78.2
	1000–1600	78.3	74.4	78.1	80.6	
SG 1stD 3–2	900–1730	76.4	77.2	79.2	83.1	78.5
	1000–1600	77.5	74.7	78.3	81.4	
SG 1stD 5–3	900–1730	75.8	76.9	79.4	81.1	78.6
	1000–1600	78.6	74.7	79.4	82.5	
SG 2ndD 3–2	900–1730	75.8	68.1	71.4	80.0	74.0
	1000–1600	75.0	71.4	71.1	78.9	
SG 2ndD 5–3	900–1730	75.8	79.2	76.9	83.3	78.8
	1000–1600	76.4	77.5	77.8	83.6	
NG 1stD 21	900–1730	80.6	76.9	79.2	83.9	79.2
	1000–1600	79.7	71.9	79.7	81.7	
NG 1stD 5	900–1730	78.9	77.8	79.2	83.6	79.1
	1000–1600	77.5	74.7	78.1	83.1	
SNV	900–1730	80.6	68.1	75.6	80.6	74.7
	1000–1600	79.4	58.6	73.9	80.8	
SNV + 1stD	900–1730	74.7	77.8	71.7	82.2	75.3
	1000–1600	77.2	63.9	72.5	82.2	
MSC	900–1730	71.1	70.6	76.9	78.9	72.3
	1000–1600	70.0	57.2	75.0	78.9	
MSC +1stD	900–1730	76.4	78.3	71.9	80.8	74.8
	1000–1600	75.6	63.6	71.9	80.0	
Normalization	900–1730	81.4	83.1	82.2	85.3	82.4
	1000–1600	81.4	82.5	80.0	83.6	
Absorbance	900–1730	83.3	60.3	83.6	85.8	77.7
	1000–1600	80.0	60.8	83.9	83.6	
Absorbance + Baseline correction	900–1730	85.3	76.4	80.6	82.5	80.8
	1000–1600	82.8	78.3	78.1	82.8	
Mean		77.8	71.8	77.7	82.2	

Table 2
Validation accuracies of single wheat kernels discrimination according to DON.

	Spectral range	LDA	Naïve Bayes	KNN	ANN	Mean
Raw spectra	900–1730	67.8	72.2	70.8	69.3	71.7
	1000–1600	75.0	72.8	70.8	75.0	
1stD	900–1730	69.4	69.2	69.4	71.4	70.4
	1000–1600	70.6	66.4	72.5	74.2	
SG 1stD 3–2	900–1730	70.8	68.9	72.8	73.1	71.1
	1000–1600	70.3	65.3	73.6	73.9	
SG 1stD 5–3	900–1730	70.3	69.2	72.5	75.3	71.2
	1000–1600	70.8	66.4	72.5	72.8	
SG 2ndD 3–2	900–1730	68.9	70.3	71.4	73.3	71.4
	1000–1600	68.9	72.8	72.8	72.5	
SG 2ndD 5–3	900–1730	70.6	71.7	72.8	68.1	71.3
	1000–1600	71.4	71.9	72.2	71.4	
NG 1stD 21	900–1730	74.2	67.2	72.8	73.3	71.9
	1000–1600	74.4	65.0	72.2	76.1	
NG 1stD 5	900–1730	71.4	67.5	71.9	67.2	69.9
	1000–1600	71.7	65.3	73.3	71.1	
SNV	900–1730	71.7	74.2	71.4	73.9	73.3
	1000–1600	71.1	76.4	71.1	76.9	
SNV + 1stD	900–1730	68.1	71.9	72.5	76.1	72.7
	1000–1600	73.1	75.0	74.7	70.6	
MSC	900–1730	69.7	75.3	71.9	76.4	73.5
	1000–1600	70.8	76.1	71.9	76.1	
MSC + 1stD	900–1730	68.6	71.9	71.9	74.4	73.1
	1000–1600	73.1	75.3	75.6	73.9	
Normalization	900–1730	73.9	71.7	72.2	73.1	72.3
	1000–1600	73.1	71.7	69.4	73.1	
Absorbance	900–1730	72.5	72.8	71.4	74.7	72.8
	1000–1600	75.6	72.8	69.4	73.1	
Absorbance + Baseline correction	900–1730	71.7	71.7	71.9	73.6	71.8
	1000–1600	75.6	73.6	65.6	70.8	
Mean		71.5	71.1	71.9	73.2	

of 0.87 and a SEP of 60.8 mg/kg. Their results would be far from naturally-contaminated DON concentrations found in the field and, thus, the application of their model would not fit with the legislation demands. Although we obtained similar adjustments (R^2 = 0.88), we focused on naturally found levels of contamination (<LOD to 135.7 mg/kg) that would be able to accurately detect high-DON contaminated kernels in terms of RMSEP (6.66 mg/kg).

Otherwise, Jin et al. (2014) estimated the correlation between the visual FDK and SK-NIR DON data obtaining a correlation of 0.68. As expected, their results were similar to our percentage of kernels which, even though they presented symptoms of fungal growth, did not contain DON and vice versa. On the other hand, Peiris, Pumphrey, and Dowell (2009) studied DON absorbance NIR spectra. The different spectral profiles from DON in acetonitrile, sound and FDK were subtracted and compared. It allowed to attributing the changes produced by fungi and DON contamination to the differences in peak intensities in specific bands. They used log (1/T) and 2nd derivative pre-processing to detect differences in the spectral peaks. For FDK, broad differences were observed at 1205 nm and around 1400 nm for 1/T and 1195 and 1425 nm for the 2nd derivative. These peaks are found in similar regions to our characteristic peaks, as 1220 and 1406 nm. Peiris et al. (2009) related the spectral peak at 1363 nm with FDK, close to the 1350 nm we obtained. Nevertheless, we should consider that their analysis was on kernels contaminated in a broader range (33–1008 mg/kg) than the one we used (<LOD-135.7 mg/kg), in which they used artificial contamination that can cause differences in position and peak intensities.

Although previous studies did not reach accurate DON predictions in single kernels, the emerging of HSI technology may permit a fast analysis of specific regions from the image, as a single kernel or even a portion, for the contamination levels. On the other hand, Tekle, Mage, Segtnan, and Bjornstad (2015) also evaluated DON contamination, although they used single oat kernels. They also worked with a spectrum for each reference value regarding an individual grain, using PLS regression to model them. Otherwise, they applied logarithmic functions to avoid non-linearities. The performance of their model reached a coefficient of determination of 0.81 and a Root Mean Square Error of Cross-Validation (RMSECV) of 39.8 mg/kg. Due to the high RMSE obtained, the authors considered HSI-NIR suitable for FDK detection in oats. On the other hand, recently published works attempted the quantification of DON using HSI but in barley or corn (Parrag et al., 2020; Su et al., 2021). However, Parrag et al. (2020) predicted the level of DON in corn homogenized samples using a ROI of 20 × 100 pixels instead of single kernels. The model performance had a RMSEP of 11.95 mg/kg using 20 PC. Despite the results showing the difficulty to predict DON, we obtained better efficiencies for SK predictions (RMSEP = 6.65 mg/kg), even using naturally contaminated samples and a broader range of contaminations. Shi, Liu, Zhao, Liu, and Zheng (2020) studies focused on the Multispectral Imaging (MSI) analysis of 105 samples of 20 wheat grains instead of individual kernels with HSI. As they were working with the mean spectra of 20 wheat kernels, reference values presented fewer deviations than for SK analysis, in which the DON differences between grains are high. Thus, they obtained accurate predictions and classifications for wheat batches. MSI has been proposed as a potential technique for DON spectral analysis that could reduce data dimension and enhance analysis speed. Thus, characteristic wavelengths selection from HSI would be a considerable strategy to reduce data dimension. Despite the recent advances in DON detection by HSI-NIR, the correctness in toxin levels prediction need to improve. Consequently, discriminant strategies won popularity for DON management with HSI strategies. In our previous works aiming the standardization of the HSI for single kernel analysis, cross-validated PLS models were used for a reduced sample set (50 kernels). The use of a reduced sample size and a cross-validation method are associated to enhanced adjustments; thus, the model presented a high performance, achieving a R^2 of 0.88 and RMSECV of 4.8 mg/kg, motivating the present work. As it was expected, increasing kernel number and using external validation, the adjustment

has decreased and the RMSEP increased, although RPD indicated excellent predictions for both models.

The correlation between *Fusarium* and DON presence with the physical and chemical changes of the cereal kernels remains a goal for cereal sorting strategies. *Fusarium* and DON analysis by NIR spectroscopy usually presents sensitivity issues that should be monitored to detect contaminated grains. However, Jin et al. (2014) correlated the visually labelled FDK and SK-NIR data, obtaining a correlation of 0.72. In addition, the higher correlation between visual symptoms and DON suggested the use of both techniques for the indirect estimation of DON in wheat (0.74). However, the correlation of SK-NIR for FDK estimation with DON falls to 0.49, which shows the difficulty of indirect detection of DON levels. Thus, classification strategies by NIR spectroscopy are more suitable than studying the correlation between fungal damage and DON.

Several authors focused on the NIR detection and classification of contamination on kernels. Singh et al. (2012) detected fungal damage on wheat kernels using NIR and colour imaging technologies. Although colour imaging obtained enhanced performances, NIR technology also gave good results, showing accuracies above 88.7%, especially in LDA models. From the full NIR spectra used by Pearson and Wicklow (2006), some wavelengths (580, 790 and 1405 nm) could describe the features of healthy and fungal infected maize with 85% and 98%, respectively. The authors also used kernels with advanced fungal symptomatology and obtained correct discrimination of 96.6%. Tallada, Wicklow, Pearson, and Armstrong (2011) categorized four levels depending on their stage of infection with LDA and multi-layer perception neural network (MLP). The reference criteria used was also according to the visual symptoms. The models could classify correctly the 89% and 79% of the control and infected kernels, respectively, which are comparable to ours (86%). All the authors cited in this section artificially inoculated fungi to their samples before NIR analysis. Consequently, the symptoms observed are sometimes more severe than using naturally contaminated samples and have to be considered when comparing the results.

In some studies, authors used different reference methods than visual inspection and artificial to detect fungi. Polder et al. (2005) quantified *Fusarium* amount on the kernel by quantitative Polymerase Chain Reaction (qPCR) analysis, avoiding the subjectivity of visual inspection, as it is specific to the fungal species of interest. The authors could correlate the spectral information with *Fusarium* DNA levels above 100 pg with a coefficient of determination of 0.8.

Hyperspectral and multispectral near-infrared spectroscopy discriminated wheat kernels according to DON levels. Chemometric methods modelled the spectral information extracted from single wheat kernels to discriminate them according to certain DON limits. There are not many studies available on the classification of wheat kernels according to DON levels. However, some authors also tried to classify cereal kernels according to different mycotoxins. Yao et al. (2013) used HSI to discriminate corn kernels according to aflatoxins levels. The spectral ranges used were the visible and the NIR, irradiating the sample with fluorescence light. Two classification models, different from the one applied in the present study and based on pixel discrimination, were implemented (maximum likelihood and binary encoding). Nevertheless, the binary encoding presented higher performance results with 87% correct classification for a 20 μg/kg threshold. The single-pixel analysis compares with the analysis of DON in oat kernels done by Tekle et al. (2015). They used PLS-DA to classify pixels according to DON with a correlation between predicted and measured values of 0.79. Following similar goals to those in the present study, some authors focused on the discrimination of DON contaminated kernels. Barbedo, Tibola, and Lima (2017) developed an algorithm based on probability functions able to discriminate the images in three different groups ($\leq$0.5 mg/kg; 0.5–1.25 mg/kg: $>$ 1.25 mg/kg). Algorithms classified wheat batches (not individual kernels) with 72% accuracy for three classes. With the cut-off fixed at 1.25 mg/kg for the discrimination into two groups, the classification accuracy rose to 81%. The results were comparable with ours, as we obtained correctness above 76%, although we used individual kernels instead of groups of around 30–50 kernels.

Instead of building classification algorithms, Alisaac et al. (2019) compared spectral signatures of kernels with different DON concentrations. They obtained correlations of $>$0.80 between the NIR spectra and DON. These high correlations in the NIR range suggest that our classifications models focused on the information contained in specific regions, which account for the changes produced by fungi when DON is present. Several studies tried the detection of mycotoxins using HSI technologies. Nevertheless, most of them analysed bulk samples or grain groups instead of single kernels. Liang et al. (2020) and Shi et al. (2020) achieved the classification of bulk wheat and groups of wheat kernels, respectively, according to DON levels. Shi et al. (2020) focused on multispectral imaging for the calibration of the PLS-DA model with an accuracy precision of 94.29%. Although wheat grains were scanned individually in the crease-up and down position, they used 20 kernel batches for calibration and validation. Conversely, Liang et al. (2020) analysed 70 grains in each sample in the NIR range. The combination of SNV, genetic algorithm and sparse autoencoder (SAE) showed their best performance, similar to the previous commented study.

In the same way as for prediction, our previous study (using cross-validated models with a reduced sample set) calibrated classification models with an accuracy up to 100% (Femenias et al., 2021). The present study reinforced these results by increasing the kernel number and validating externally the models with different kernels than the calibration. Thus, the results achieved are more realistic, avoiding the over-fitting of the cross-validated models.

Shen et al. (2022) focused on DON prediction of wheat individual kernels using a similar methodology of this study, although they inoculated artificially *Fusarium graminearum* in the field. The concentration range used went from n.d. to 507.3 mg/kg, thus the RMSEP for the PLS model was 46.3 mg/kg with an RPD of 1.92. Despite the RMSEP is not directly comparable with the present study due to the differences of the contamination range, the RPD is quite lower than the obtained in the present study (3.21). In addition, the classification of kernels according to symptomatology reached accurate results, with classification accuracies from 93.3 to 100%. In artificially inoculated wheat, the symptomatology of kernels is visually more noticeable than for naturally contaminated kernels, what could explain the higher accuracy.

Despite the predictive and classification performances are not perfect, the application of HSI-NIR would be interesting as a mitigation strategy. The on-line application of models should be based on the classification models focused on the removal of the contaminated kernels fraction of the wheat batch. The models could detect and remove more than 75% of the contaminated kernels, reducing the overall contamination. However, for a rapid and reliable acquisition of data for on-line application the data dimensionality and processing time should be reduced. Consequently, new advances will require the calibration of algorithms which automatically select the wavelengths regions or the wavelengths with the highest relevance on the model, pre-treatment application and data processing. Considering the methodology already applied in industry for the high speed detection of colour features of grains (Delwiche, 2008; Pearson, 2010), e.g. removal of the non-white rice grains by air ejectors, the hyperspectral imaging would go beyond the colour and textural parameters to detect 'invisible' chemicals from cereal samples and remove them with similar techniques. Consequently, the detection of the contaminated kernels would activate the air ejectors, removing the contaminated fraction of the batch and reducing the overall contamination.

5. Conclusions

HSI-NIR analysis of wheat individual kernels presented differences in the spectral profile from fungal and DON contaminated and non-contaminated grains. The differences in spectral intensities, especially between the 1100–1400 nm, could be correlated to the symptomatology

caused by Fusarium growth on wheat kernels, and consequently, with an indirect DON prediction. However, the changes produced in the cereal chemical composition due to fungal growth, like proteins, carbohydrates and lipids, could be indirectly related with DON presence on wheat kernels. DON quantification results show too high prediction errors to quantify DON at EU legal limits. Consequently, the authors focused on the discrimination of infected kernels as a more convenient mitigation approach. According to the results, it was proven that the classification strategies are more suitable for fungi and DON management in cereals than for their quantification, obtaining discrimination accuracies according to the EU cut-off around 86% and 77%, respectively. Thus, the detection of the low percentage of highly contaminated kernels inside a batch would be a key mitigation strategy for contaminated cereals.

CRediT authorship contribution statement

Antoni Femenias: Conceptualization, Methodology, Software, Formal analysis, Data curation, Writing – original draft, Validation, Writing – review & editing. **Enric Llorens-Serentill:** Methodology, Software, Formal analysis, Data curation. **Antonio J. Ramos:** Writing – original draft, Validation, Writing – review & editing, Resources, Visualization, Supervision. **Vicente Sanchis:** Writing – original draft, Validation, Writing – review & editing, Supervision, Project administration, Funding acquisition. **Sonia Marín:** Conceptualization, Methodology, Software, Formal analysis, Data curation, Writing – original draft, Validation, Writing – review & editing, Supervision, Project administration, Funding acquisition.

Acknowledgements

This work was supported by Project AGL2017-87755-R funded by MCIN/AEI/10.13039/501100011033/FEDER "Una manera de hacer Europa" and project PID2020-114836RB-I00 funded by MCIN/AEI/10.13039/501100011033. The authors are grateful to the University of Lleida (predoctoral grant).

Appendix A. Supplementary data

Supplementary data to this article can be found online at https://doi.org/10.1016/j.foodcont.2022.109239.

References

Agelet, L. E., & Hurburgh, C. R. (2010). A tutorial on near infrared spectroscopy and its calibration. *Critical Reviews in Analytical Chemistry, 40*(4), 246–260. https://doi.org/10.1080/10408347.2010.515468

Alisaac, E., Behmann, J., Rathgeb, A., Karlovsky, P., Dehne, H. W., & Mahlein, A. K. (2019). Assessment of Fusarium infection and mycotoxin contamination of wheat kernels and flour using hyperspectral imaging. *Toxins, 11*(10), 1–18. https://doi.org/10.3390/toxins11100556

AOAC. (2005). Official methods of analysis. *Official Methods of Analysis of AOAC International, 18*, 20877–22417.

Barbedo, J. G. A., Tibola, C. S., & Fernandes, J. M. C. (2015). Detecting Fusarium head blight in wheat kernels using hyperspectral imaging. *Biosystems Engineering, 131*, 65–76. https://doi.org/10.1016/j.biosystemseng.2015.01.003

Barbedo, J. G. A., Tibola, C. S., & Lima, M. I. P. (2017). Deoxynivalenol screening in wheat kernels using hyperspectral imaging. *Biosystems Engineering, 155*, 24–32. https://doi.org/10.1016/j.biosystemseng.2016.12.004

Champeil, A., Fourbet, J. F., & Doré, T. (2004). Effects of grain sampling procedures on Fusarium mycotoxin assays in wheat grains. *Journal of Agricultural and Food Chemistry, 52*(20), 6049–6054. https://doi.org/10.1021/jf049374s

Delwiche, S. R. (2008). High-speed bichromatic inspection of wheat kernels for mold and color class using high-power pulsed LEDs. *Sensing and Instrumentation for Food Quality and Safety, 2*(2), 103–110. https://doi.org/10.1007/s11694-008-9037-1

Delwiche, S. R., Kim, M. S., & Dong, Y. (2011). Fusarium damage assessment in wheat kernels by Vis/NIR hyperspectral imaging. *Sensing and Instrumentation for Food Quality and Safety, 5*(2), 63–71. https://doi.org/10.1007/s11694-011-9112-x

Delwiche, S. R., Pearson, T. C., & Brabec, D. L. (2007). High-speed optical sorting of soft wheat for reduction of deoxynivalenol. *Plant Disease, 89*(11), 1214–1219. https://doi.org/10.1094/pd-89-1214

Delwiche, S. R., Rodriguez, I. T., Rausch, S. R., & Graybosch, R. A. (2019). Estimating percentages of Fusarium-damaged kernels in hard wheat by near-infrared hyperspectral imaging. *Journal of Cereal Science, 87*, 18–24. https://doi.org/10.1016/j.jcs.2019.02.008

Dowell, F. E., Ram, M. S., & Seitz, L. M. (1999). Predicting scab, vomitoxin, and ergosterol in single wheat kernels using near-infrared spectroscopy. *Cereal Chemistry, 76*(4), 573–576. https://doi.org/10.1094/CCHEM.1999.76.4.573

European Commission. (2006a). Commission Regulation (EC) No 1881/2006 of 19 December 2006. Setting maximum levels for certain contaminants in foodstuffs. *Official Journal of the European Communities, 364*(1881), 5–24.

European Commission. (2006b). Commission regulation (EC) N° 401/2006 of 23 February 2006. Laying down the methods of sampling and analysis for the official control of the levels of mycotoxins in foodstuffs. *Official Journal of the European Union, 70*(401), 12–34.

Femenias, A., Bainotti, M. B., Gatius, F., Ramos, A. J., & Marín, S. (2021). Standardization of near infrared hyperspectral imaging for wheat single kernel sorting according to deoxynivalenol level. *Food Research International, 139* (November 2020), Article 109925. https://doi.org/10.1016/j.foodres.2020.109925

Jaillais, B., Roumet, P., Pinson-gadais, L., & Bertrand, D. (2015). Detection of Fusarium head blight contamination in wheat kernels by multivariate imaging. *Food Control, 54*, 250–258. https://doi.org/10.1016/j.foodcont.2015.01.048

Jin, F., Bai, G., Zhang, D., Dong, Y., Ma, L., Bockus, W., et al. (2014). Fusarium-damaged kernels and deoxynivalenol in Fusarium-infected U.S. winter wheat. *Phytopathology, 104*(9), 472–478. https://doi.org/10.1094/PHYTO-07-13-0187-R

Liang, K., Huang, J., He, R., Wang, Q., Chai, Y., & Shen, M. (2020). Comparison of Vis-NIR and SWIR hyperspectral imaging for the non-destructive detection of DON levels in Fusarium head blight wheat kernels and wheat flour. *Infrared Physics & Technology, 106*, Article 103281. https://doi.org/10.1016/j.infrared.2020.103281

Liang, K., Liu, Q. X., Xu, J. H., Wang, Y. Q., Okinda, C. S., & Shena, M. X. (2018). Determination and visualization of different levels of deoxynivalenol in bulk wheat kernels by hyperspectral imaging. *Journal of Applied Spectroscopy, 85*(5), 953–961. https://doi.org/10.1007/s10812-018-0745-y

Marroquín-Cardona, A. G., Johnson, N. M., Phillips, T. D., & Hayes, A. W. (2014). Mycotoxins in a changing global environment - a review. *Food and Chemical Toxicology, 69*, 220–230. https://doi.org/10.1016/j.fct.2014.04.025

Parrag, V., Gillay, Z., Kovács, Z., Zitek, A., Böhm, K., Hinterstoisser, B., … Baranyai, L. (2020). Application of hyperspectral imaging to detect toxigenic Fusarium infection on cornmeal. *Progress in Agricultural Engineering Sciences, 16*(1), 51–60. https://doi.org/10.1556/446.2020.00009

Paul, P. A., Lipps, P. E., & Madden, L. V. (2005). Relationship between visual estimates of Fusarium head blight intensity and deoxynivalenol accumulation in harvested wheat grain: A meta-analysis. *Phytopathology, 95*(10), 1225–1236. https://doi.org/10.1094/PHYTO-95-1225

Pearson, T. (2010). High-speed sorting of grains by color and surface texture. *Applied Engineering in Agriculture, 26*(3), 499–505.

Pearson, T. C., & Wicklow, D. T. (2006). Detection of corn kernels infected by fungi. *Transactions of the ASABE, 49*(4), 1235–1245. https://doi.org/10.13031/2013.21723

Peiris, K. H. S., Bockus, W. W., & Dowell, F. E. (2016). Near-infrared spectroscopic evaluation of single-kernel deoxynivalenol accumulation and Fusarium Head Blight resistance components in wheat. *Cereal Chemistry Journal, 93*(1), 25–31. https://doi.org/10.1094/CCHEM-03-15-0057-R

Peiris, K. H. S., Pumphrey, M. O., Dong, Y., Maghirang, E. B., Berzonsky, W., & Dowell, F. E. (2010). Near-infrared spectroscopic method for identification of Fusarium head blight damage and prediction of deoxynivalenol in single wheat kernels. *Cereal Chemistry, 87*(6), 511–517. https://doi.org/10.1094/CCHEM-01-10-0006

Peiris, K. H. S., Pumphrey, M. O., & Dowell, F. E. (2009). NIR Absorbance characteristics of deoxynivalenol and of sound and Fusarium-damaged wheat kernels. *Journal of Near Infrared Spectroscopy, 17*(4), 213–221. https://doi.org/10.1255/jnirs.846

Polder, G., van der Heijden, G. W. A. M., Waalwijk, C., & Young, I. T. (2005). Detection of Fusarium in single wheat kernels using spectral imaging. *Seed Science & Technology, 33*(3), 655–668. https://doi.org/10.15258/sst.2005.33.3.13

Ropelewska, E., & Zapotoczny, P. (2018). Classification of fusarium-infected and healthy wheat kernels based on features from hyperspectral images and flatbed scanner images: A comparative analysis. *European Food Research and Technology, 244*(8), 1453–1462. https://doi.org/10.1007/s00217-018-3059-7

Sauer, D. B. (1988). Effects of fungal deterioration on grain: Nutritional value, toxicity, germination. *International Journal of Food Microbiology, 7*(3), 267–275. https://doi.org/10.1016/0168-1605(88)90045-1

Shen, G., Cao, Y., Yin, X., Dong, F., Xu, J., Shi, J., et al. (2022). Rapid and nondestructive quantification of deoxynivalenol in individual wheat kernels using near-infrared hyperspectral imaging and chemometrics. *Food Control, 131*(June 2021), Article 108420. https://doi.org/10.1016/j.foodcont.2021.108420

Shi, Y., Liu, W., Zhao, P., Liu, C., & Zheng, L. (2020). Rapid and nondestructive determination of deoxynivalenol (DON) content in wheat using multispectral imaging (MSI) technology with chemometric methods. *Analytical Methods, 12*(26), 3390–3396. https://doi.org/10.1039/d0ay00859a

Singh, C. B., Jayas, D. S., Paliwal, J., & White, N. D. G. (2012). Fungal damage detection in wheat using short-wave near-infrared hyperspectral and digital colour imaging. *International Journal of Food Properties, 15*(1), 11–24. https://doi.org/10.1080/10942911003687223

Sudakin, D. L. (2003). Trichothecenes in the environment: Relevance to human health. *Toxicology Letters, 143*(2), 97–107. https://doi.org/10.1016/S0378-4274(03)00116-4

Su, W.-H., Yang, C., Dong, Y., Johnson, R., Page, R., Szinyei, T., … Steffenson, B. J. (2021). Hyperspectral imaging and improved feature variable selection for automated determination of deoxynivalenol in various genetic lines of barley kernels

for resistance screening. *Food Chemistry, 343*(June 2020), Article 128507. https://doi.org/10.1016/j.foodchem.2020.128507

Tallada, J. G., Wicklow, D. T., Pearson, T. C., & Armstrong, P. R. (2011). Detection of fungus-infected corn kernels using near-infrared reflectance spectroscopy and color imaging. *Transactions of the ASABE, 54*(3), 1151–1158. https://doi.org/10.13031/2013.37090

Tekle, S., Mage, I., Segtnan, V. H., & Bjornstad, A. (2015). Near-infrared hyperspectral imaging of Fusarium-damaged oats (Avena sativa L.). *Cereal Chemistry, 92*(1), 73–80. https://doi.org/10.1094/CCHEM-04-14-0074-R

Yao, H., Hruska, Z., Kincaid, R., Brown, R. L., Bhatnagar, D., & Cleveland, T. E. (2013). Hyperspectral image classification and development of fluorescence index for single corn kernels infected with Aspergillus flavus. *Transactions of the ASABE, 56*(5), 1977–1988. https://doi.org/10.13031/trans.56.10091